Surface Quality Analysis After Face Grinding of Ceramic Shafts Characterized by Various States of Sintering

Marcin Żółkoś[1], Roman Wdowik[1(✉)], R. M. Chandima Ratnayake[2], Witold Habrat[1], and Janusz Świder[3]

[1] The Faculty of Mechanical Engineering and Aeronautics, Rzeszow University of Technology, 35-959 Rzeszów, Poland
rwdowik@prz.edu.pl
[2] The Department of Mechanical and Structural Engineering and Materials Science, University of Stavanger, 4036 Stavanger, Norway
[3] Ceramic Department CEREL, Institute of Power Engineering, 36-040 Boguchwała, Poland

Abstract. The article concerns an investigation of surface roughness in relation to different characteristics of ceramic material. Three different levels of temperature (1320 °C, 1490 °C and 1620 °C) have been used to sinter the ceramic in the preparation of samples. The machining has been performed using a computer numerical control (CNC) milling machine, together with a face grinding wheel, specific face grinding strategy, and special work holding arrangement. The surface roughness is assessed using three parameters (Ra, Rz, Rsm). The contact measurements of surface roughness were carried out using the 3D MahrSurf XR 20 profilometer. The surfaces of machined samples were also analyzed using the InfiniteFocus Real3D microscope, in order to determine the influence of the selected machining strategy on the machined surfaces. The values of the selected roughness parameters were recorded depending on the material and its degree of sintering. The selected machining strategy, for all the analyzed ceramic samples (i.e. in relation to states of sintering), allowed Ra parameter values below 0.43 μm, Rz below 3.5 μm and Rsm below 50 μm, respectively, to be obtained.

Keywords: Grinding · Ceramic materials · Surface roughness · Sintering temperature

1 Introduction

The shaping of ceramic materials is a complex and multi-stage process. The basic stages of product development include: preparation of ceramic powders, forming, sintering and machining [1]. The preparation of ceramic powders focuses on the required chemical composition including adhesives, which facilitate the forming process. The forming process (carried out e.g. by isostatic pressing) leads to a (blank) product.

Machining of products after forming is defined as machining in the green state. Industrial firms usually use cutting tools for the needs of such a process. Grinding

B. Gapiński et al. (Eds.): *Advances in Manufacturing II* - Volume 4, LNME, pp. 329–341, 2019.
https://doi.org/10.1007/978-3-030-16943-5_29

wheels may also be used, but ceramic material adheres to the tool's surface, decreasing cutting ability and process performance. In order to perform machining processes of ceramic materials, cutting tools made of cemented carbides or diamond cutting tools are usually used. It is also possible to use high-speed steels, but the tool life is very limited in this case [2, 3].

The next stage in the production of ceramic products concerns sintering. The sintering process influences the properties of the material. It increases material hardness and decreases porosity and absorptivity. The sintering process also causes material shrinkage. Pre-sintered ceramics (defined as the white state) can be machined using cutting tools with diamond inserts or diamond grinding wheels, depending on the temperature of sintering [4, 5]. As the result of further sintering and the formation of the bonds between the ceramic particles, the ceramic material characterized by the highest possible hardness is obtained (the final sintered material). The machining process of ceramic material in this state can be carried out using super-abrasive tools – mainly metal, resin and vitrified grinding wheels. Diamond or cubic boron nitride (CBN) grains are used as an abrasive material [6].

The grinding process, in the final sintering state, leads to the specific surface structure of the ceramic product (e.g. unique surface roughness). The machining process of ceramic materials which contain conductive phases, such as Al_2O_3-Ti(C,N)-TiB_2 or Si_3N_4-TiB_2, can also be run as electro discharge machining [7]. Moreover, laser machining [8], hybrid machining (e.g. laser assisted machining) [9, 10] or abrasive waterjet machining [11] processes are applied. Ultrasonic machining also plays an important role in the shaping of ceramic materials [12].

Modern ceramic materials are used in the design of many products such as: bushings, guide rollers, nozzles, hydrocyclones, valve parts, insulators, implants, etc. [1, 13–15]. Ceramic materials are also employed in the production of cutting inserts used in the machining processes of superalloys, cast irons and hardened materials [16].

An analysis of the surface quality after the grinding process is an interesting research topic. In paper [17], Musiał studied the influence of process parameters on the values of surface texture parameters. Wdowik et al. [18] presented the results of measurements of surface roughness parameters after ultrasonic assisted grinding. The work [19] of Qu et al. presents the results of surface quality measurements after the machining of ceramic composites.

The following questions should be answered to better understand the machinability of ceramic products:

1. Does the material and its degree of sintering significantly influence the surface roughness?
2. Can similar machining parameters be applied for every material and its sintering states, in order to achieve similar surface roughness?
3. Is it possible to obtain the required shape accuracy using frequently used machining strategies – e.g. face grinding?

The article is an attempt to answer these questions. For this purpose, the influence of the type of ceramic material and the sintering state on selected surface roughness parameters (Ra, Rz, Rsm) was investigated for the unique machining strategy used by

an industrial partner. This machining strategy leads to a significant reduction in machining time.

2 Research Methodology and Experimental Conditions

Samples in the form of cylinders (diameter of 16 mm and length of 100 mm), made of four different ceramic materials, were used as the workpieces in the conducted experiments. The samples were obtained after the sintering of four ceramic materials at three different temperatures in the following furnaces: Bickley 5000 (temperatures: 1250 and 1320 °C), Estherm SIN 36-1550 (1490 °C) and Riedhammer 150/4V/180 (1620 °C). Twelve different types of samples were finally obtained. Three identical samples were made for each variant, so the total number of samples used for investigation was 36. The abovementioned materials (refer to Table 1) were machined and measured using the same machining and measurement parameters, which are presented in Table 2. The sintering temperatures for Y-TZP ceramic material differ, due to the lower temperature of the final sintering process (1490 °C). Therefore, it is the highest sintering temperature for this type of ceramic material; above this value, no change in the material hardness or porosity can be observed.

Table 1. Properties of used ceramic materials which are obtained as a result of research carried out according to PN-EN 60672-2 p.5; IEn-8/2002/IEn-BL-F.

Designation of ceramic material	Sintering temperature, °C	Apparent porosity, %	Water absorption, %	Apparent density, g/cm^3	The use of ceramics
Y-TZP	1250	25.77	5.71	4.52	Structural ceramics, wear resistant parts, thread, wire and roller guides, thermal barrier coatings, fiber optic ferrules and sleeves, oxygen sensors, precision ball valves, balls and seats, rollers and guides for metal tube forming, hot metal extrusion dies, solid oxide fuel cell components [20, 21], scissors, cutlery, knives, hair clippers, sliding parts (e.g. in chemical pumps), grinding media, tweezers, adjusters and diesel engine parts [22, 23]
Y-TZP	1320	4.68	0.86	5.43	
Y-TZP	1490	0.04	0.01	6.09	
C795	1320	30.45	11.12	2.74	Heavy-duty forming tools, substrates and resistor cores, tiles for wear protection and ballistics, thread guides, seal and regulator discs for water taps and valves, heat-sinks for lighting systems, protection tubes in thermal processes or catalyst carriers; protection tubes and insulating tubes used in manufacturing devices for temperature measurement and control [24]
C795	1490	7.58	2.16	3.51	
C795	1620	0.06	0.02	3.88	
C799	1320	21.4	6.96	3.07	
C799	1490	4.31	1.18	3.92	
C799	1620	0.06	0.02	4.52	
MgPSZ	1320	10.93	2.08	4.95	Tools for wire forming, auxiliaries in welding processes, crowns and bridges in the dental industry, insulating rings in thermal processes, oxygen measurement cells in lambda probes [24], balls, seats, plugs, discs, liners for severe duty valves; tooling, rolls, dies, wear guides in metal processing; can seaming rolls; wear liners, cyclone liners and chokes for the mineral industry; bearings inserts and sleeves for the abrasive materials industry; wear rings and bushes for severe duty slurry pumps [25]
MgPSZ	1490	0.02	0	5.71	
MgPSZ	1620	0.01	0	5.66	

2.1 The Grinding Process

The experimental part of the research (mechanical machining) was carried out using the CNC test stand, which was developed for the needs of the research grant regarding high-performance machining of ceramic materials with ultrasonic assistance [26]. The test stand is used in the Ceramic Department CEREL for further research [14]. The machining strategy was selected based on industrial practice, in order to shorten machining time. Due to the relatively low feed rates used in the grinding processes of ceramic materials, the final machining time can be controlled by the length of the programmed tool path. Therefore, the tests were carried out for face grinding with the use of a resin-bonded diamond grinding wheel. The workpiece rotated around its axis (see Fig. 1). This strategy allows the removal of the whole machining allowance, by moving the grinding wheel only to the center of the workpiece. The strategy may influence the machining time significantly, especially in the case of workpieces characterized by relatively large diameters.

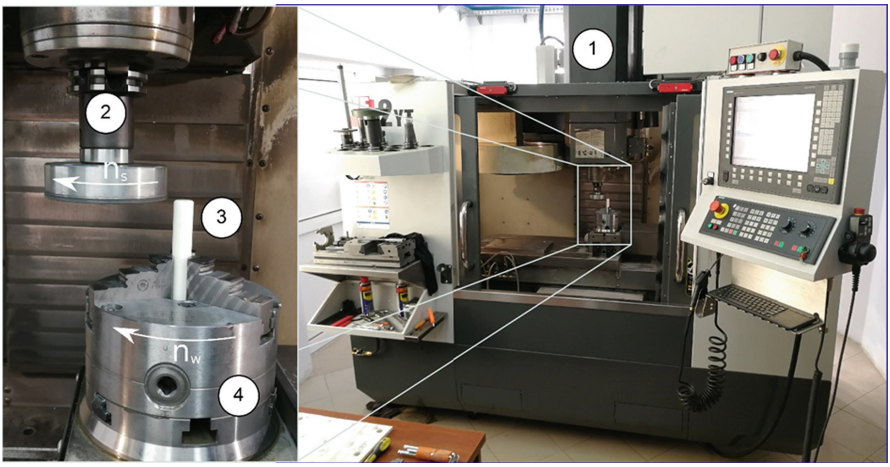

Fig. 1. Configuration of the test stand: 1 – machine tool, 2 – diamond grinding wheel, 3 – workpiece, 4 – rotary table (4^{th} axis).

Table 2. Parameters of machining and measurement processes.

Parameters of grinding process	Parameters of surface roughness measurement
Face grinding wheel Urdiamant 16-4992 6A2 1-100-6/4 B-IIIK D64 K100 5% synthetic coolant mixed with water Grinding speed, v_c = 38 m/s Feed rate, v_f = 5 mm/min Grinding depth, a_e = 0.03 mm Rotational speed of the workpiece, n_w = 20 rev/min	Lt = 1.5 mm Ls = 2.5 µm Lc = 0.25 mm VB = ±250 µm Vt = 0.5 mm/s Points = 3000 Head: MFW-250:1 (#1854) 0.1% Feed mechanism: drive unit GD 120

2.2 Measurements of Surface Roughness Parameters

The measurements of surface roughness parameters were performed with the use of the 3D MahrSurf XR 20 profilometer in the Laboratory of Technical Metrology at the Department of Manufacturing Techniques and Automation of Rzeszow University of Technology (see Fig. 2). Measurements were performed for all 36 abovementioned samples, made of four different materials characterized by the different states of sintering (three sintering states for each material). Eight replications of single measurements of the analyzed surface roughness parameters were carried out for every sample, using a random sample position in relation to the direction of measurement. A total number of replications was 24 for the three samples characterized by the same material and sintering state. Single surface roughness measurements totaling 288 were made for all the ceramic samples (refer to the materials presented in Table 1). The surfaces of the samples were also scanned using the InfiniteFocus Real3D microscope, which is produced by the Austrian company, Alicona, and available in the abovementioned laboratory of Rzeszow University of Technology.

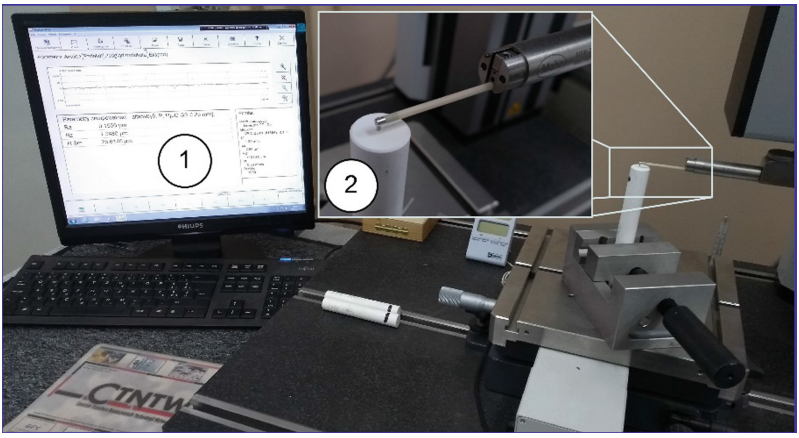

Fig. 2. MahrSurf XR 20 profilometer applied in contact measurements of surface roughness parameters as the test stand: 1 – the software and the exemplary results, 2 – the measurement of ceramic workpiece.

3 The Results of the Study

Figure 3 presents average values of the Ra parameter and the calculated confidence intervals for 24 measurements of the same type of material. The applied significance level was 0.05. The obtained values of the Ra parameter indicate statistically significant differences in surface roughness among materials with different sintering states. The

lowest values were obtained for the Y-TZP ceramic material, which was sintered at 1250 °C, and the highest ones for the C795 ceramic material sintered at the lowest temperature (1320 °C). In the case of the C799 and Y-TZP materials, the higher the sintering temperature, the higher the roughness parameter Ra. For other two materials (C795 and MgPSZ), the lowest values of parameter Ra were measured for the sintering temperature of 1490 °C. However, in the other two sintering states, the measured Ra parameter assumed higher values.

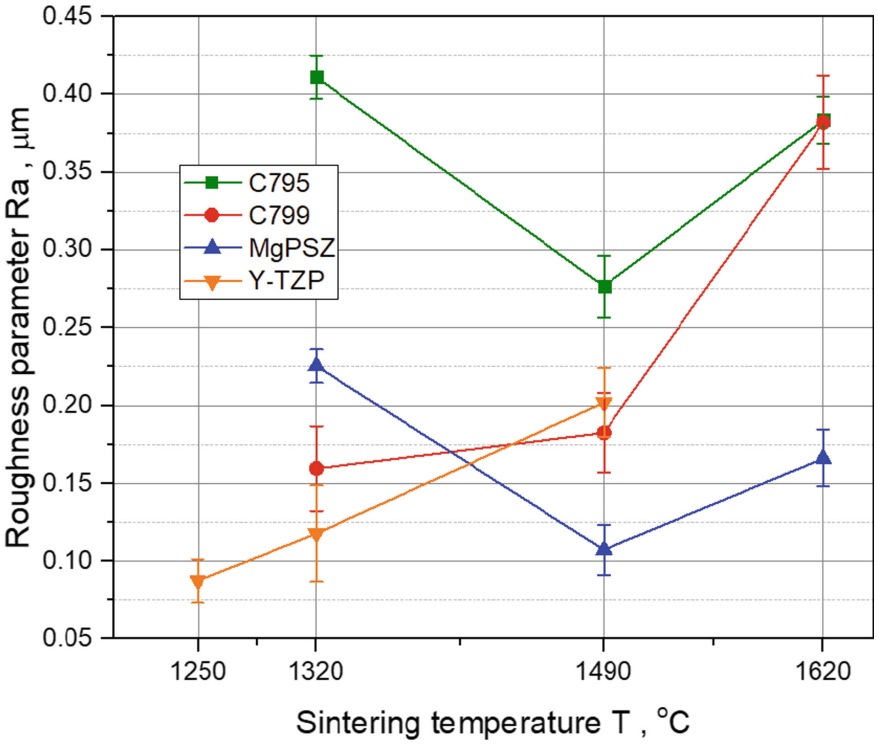

Fig. 3. The results of Ra parameter measurements vs. sintering temperature.

Figure 4 indicates average values of the Rz parameter and calculated confidence intervals for 24 measurements of the same type of material. The applied significance level was 0.05. The lowest values were obtained for the Y-TZP material sintered at 1250 °C and the highest for the C799 material at the highest sintering temperature of 1620 °C. Due to the well-known correlation of the Rz parameter with the Ra parameter, dependences of the Rz parameter on sintering temperature, similar to those mentioned in the previous paragraph, were observed for individual materials.

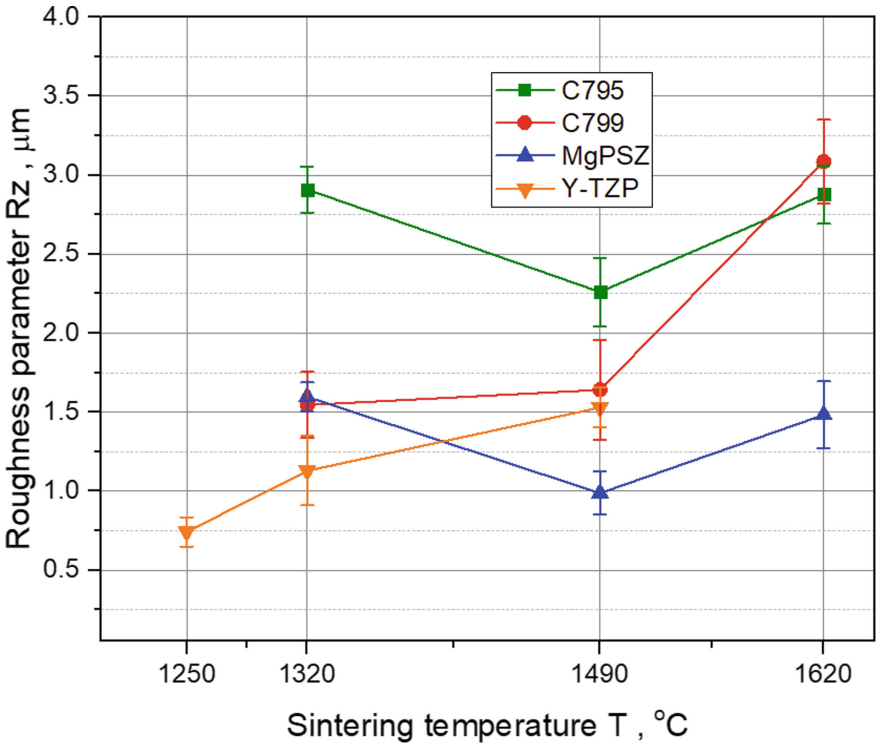

Fig. 4. The results of Rz parameter measurements vs. sintering temperature.

Figure 5 shows the mean values of the Rsm roughness parameter and the confidence intervals calculated for 24 measurements at the significance level of 0.05. The lowest values were obtained for the C795 and Mg-PSZ ceramic materials sintered at 1320 °C and the highest for the Y-TZP ceramic sintered at temperatures 1320 and 1490 °C, respectively. The values of the Rsm parameter for the materials C795 and Mg-PSZ were higher when the sintering temperature was higher. The measurements of ceramic material C799 reveal comparable values of the Rsm parameter for both 1320 and 1490 °C sintering temperatures. The values of the Rsm roughness parameter for the Y-TZP material are also characterized by such dependence.

Scans of the surfaces were also obtained using the InfiniteFocus Real3D optical microscope. Characteristic structures of the machined surfaces were observed for all

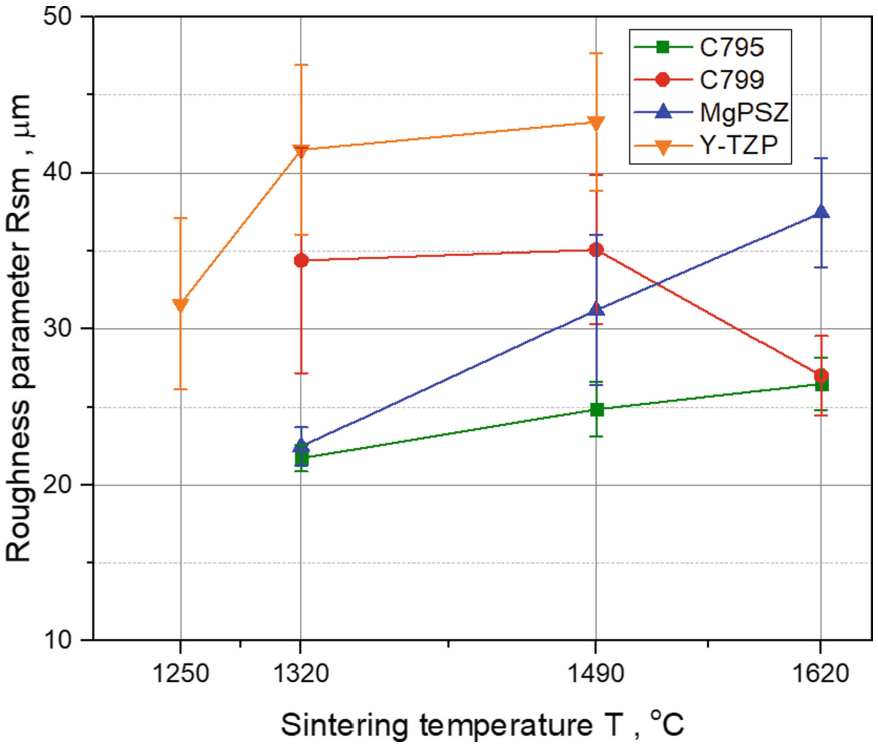

Fig. 5. The results of Rsm parameter measurements vs. sintering temperature.

samples (Fig. 6). Traces visible outside the blue circle in Fig. 6 are the result of the selected machining kinematics and, more precisely, the influence of the rotational movement of the grinding wheel and the workpiece, as well as the feed rate. The surface structure outside the blue circle is a preferable one and should cover the entire surface. Traces at the center of the machined surface (blue circle in Fig. 6) are the result of the applied machining strategy. In the selected strategy, in order to shorten the machining time as much as possible, the edge of the grinding wheel only approached the axis of the machined part. This resulted in mapping of the grinding wheel active surface on the sample's surface, which is manifested by traces characterized by the width equal to the width of the diamond layer on the grinding wheel (blue circle in Fig. 6). Moreover, at the place where the grinding wheel leaves the machined surface, additional traces, indicated by the red ellipse in Fig. 6, appear.

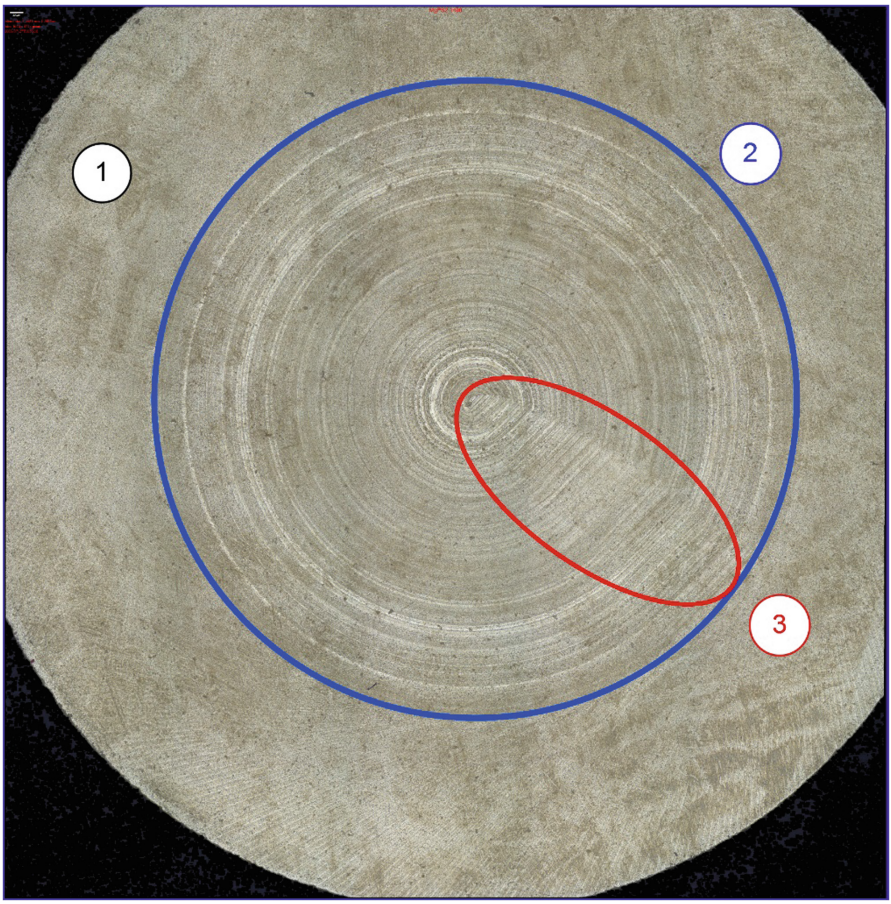

Fig. 6. The 3D scan of surface for the MgPSZ ceramic material (1490 °C): 1 - surface after the pass of the entire diamond layer of the grinding wheel's face, 2 - the grinding wheel active surface mapped on the surface of the sample, 3 - traces created as a result of the grinding wheel's retraction from the machined surface.

The cross-section of the scanned surface was also calculated using the microscope's software tool to obtain the profile of the machined face of the workpiece (Fig. 7). The negative influence of tool wear for the selected machining strategy on the surface flatness after machining was observed. The obtained profile can be explained by tool wear, which gradually increases in the following tool passes, and the machining allowance is not removed while the axis of the workpiece is approached by the theoretical edge of a grinding wheel. This is due to the wear of the grinding wheel from the outer edge to the inner edge, taking into account the direction of feed. For all ceramic samples, the highest measured value of the distance between the highest and lowest point of the cross-section profile was close to 0.08 mm.

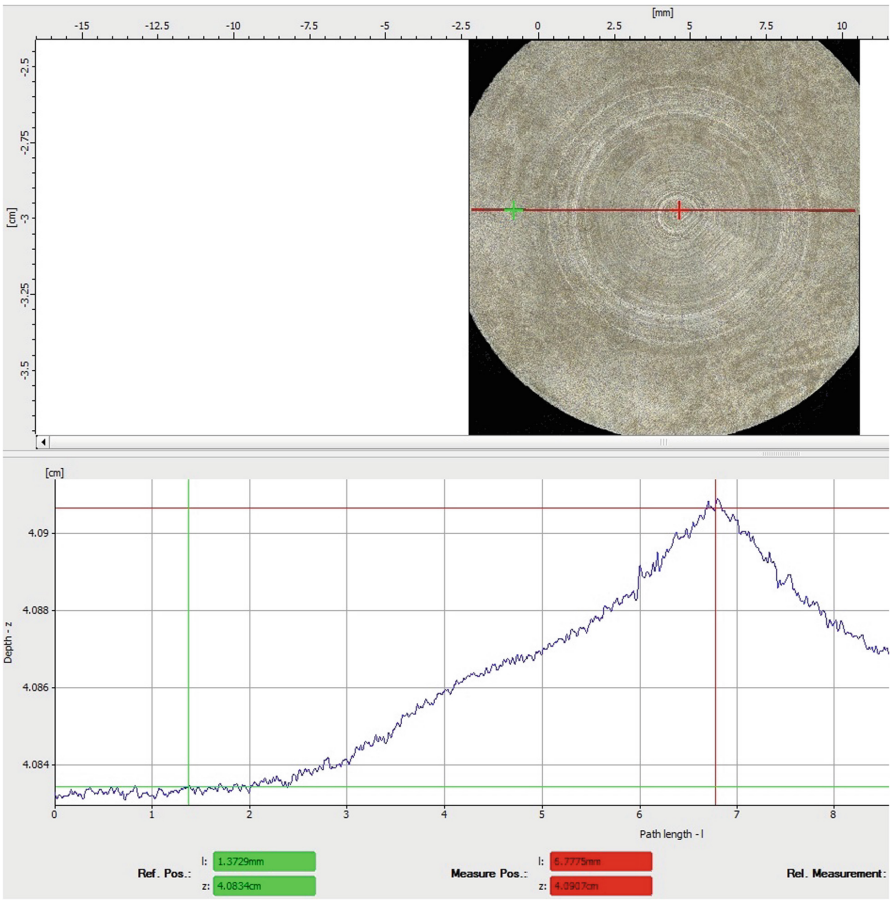

Fig. 7. Exemplary measurement of the distance (on the face of the machined workpiece) between the highest and lowest points of the profile in the cross-section of the MgPSZ (1490 °C) sample made on an InfiniteFocus Real3D microscope – result 0.07 mm.

4 Discussion

The material removal mechanism in brittle material, like ceramics machining, is achieved through microfracture and the subsequent removal of the chips by the succeeding passing grain. During the face grinding, factors, such as the wheel bond, shape of abrasive, grit concentration, depth of cut, coolant flow, etc., influence the final surface finish. Hence, the correct choice for each of these parameters is critical when grinding ceramic material with different characteristics. The sub-optimal choice of grinding parameters results in significant damage to the workpiece, the diamond wheel, or both. Damage to the ceramic workpiece is reflected as the level of surface finish that may result in premature failure in operation, as microcracks propagate under operational stress. Figures 3, 4 and 5 indicate the influence of material characteristics via

sintering temperature vs. surface roughness parameters. The shape of the plot of sintering temperature vs. roughness average of different ceramic materials shows a similar kind of change in surface roughness. Hence, it may be worth dividing the four ceramic materials into two groups. For instance, it could be concluded that the C799 and Y-TZP materials have a relatively different influence on the surface roughness, compared to that of the C795 and MgPSZ materials.

In Fig. 5, it is possible to observe quite wide confidence intervals, compared to the other charts. This may be due to the roughness measurement strategy and the occurrence of two zones with various traces after machining on the measured surface (see Fig. 6).

It would be possible to overcome the negative effects of tool wear and mapping of the grinding wheel active surface on the machined surface (at the expense of a longer machining time, albeit still shorter than using the conventional strategy), by extending the tool path by the width of a diamond layer on the grinding wheel (half of the blue circle diameter in Fig. 6).

5 Conclusion

As the result of the study, the values of the roughness parameters, Ra, Rz and Rsm, were obtained for four different ceramic materials characterized by different sintering states. The obtained results allow the following conclusions to be formulated:

- The selected combination of technological parameters, machining kinematics and tools allows (for grinding of the face of cylindrical ceramic workpieces) sufficient surface roughness (indicated by the needs of the industrial partner) to be obtained.
- The applied grinding strategy allows the values of roughness parameters, Ra below 0.45 μm, Rz below 3.5 μm and Rsm below 50 μm, to be obtained for the used materials characterized by the different sintering states.
- Clear trends, presenting the dependence of the sintering temperature on surface roughness, can be obtained after extended experiments, in which more sintering temperatures will be used.
- The use of the selected grinding strategy allows a reduction in the machining time (for a workpiece diameter of 16 mm) to 5 min and 54 s, compared to 8 min and 48 s for conventional grinding with a stationary workpiece (for larger diameters, the difference will be greater).
- The limitation of the path length in the selected machining strategy causes surface irregularity, due to the mapping of the grinding wheel active surface on the machined surface.
- In the employed machining strategy, wear of the grinding wheel has a negative effect on the flatness of the surface being machined, but the strategy is used by the industrial partner because of time savings.

Acknowledgments. The results of the presented research were obtained in 2018 after the research project entitled “Technology of high performance machining with ultrasonic assistance of geometrically complex ceramic parts” funded by The National Centre for Research and

Development in the Applied Research Programme (contract number PBS2/B6/17/2013). The study was performed thanks to the existence of the advanced test stand (machine tool), which was developed under the mentioned project, and existing collaboration between scientific and industrial partners. The investigation was partly performed as the statutory activity at Rzeszow University of Technology (grant no. DS/M.MO.18.009).

References

1. Oczoś, K.: Shaping of technical ceramic materials. Rzeszów. Publishing House, Rzeszow University of Technology (1996). (in Polish)
2. Scheller, W.L.: Conventional machining of green aluminum/aluminum nitride ceramics. Ohio J. Sci. **94**(5), 151–154 (1994)
3. Dhara, S., Su, B.: Green machining to net shape alumina ceramics prepared using different processing routes. Int. J. Appl. Ceram. Technol. **2**(3), 262–270 (2005)
4. Li, J.-Z., Wu, T., Yu, Z.-Y., Zhang, L., Chen, G.-Q., Guo, D.-M.: Micro machining of pre-sintered ceramic green body. J. Mater. Process. Technol. **212**(3), 571–579 (2012)
5. Yan, B.H., Huang, F.Y., Chow, H.M.: Study on the turning characteristics of alumina-based ceramics. J. Mater. Process. Technol. **54**(1), 341–347 (1995)
6. Webster, J., Tricard, M.: Innovations in abrasive products for precision grinding. CIRP Ann. **53**(2), 597–617 (2004)
7. Putyra, P., Laszkiewicz-Łukasik, J., Podsiadło, M., Krzywda, T.: Ceramics machining methods. Mechanik **88**(2), 120–122 (2015)
8. Samant, A.N., Dahotre, N.B.: Laser machining of structural ceramics—a review. J. Eur. Ceram. Soc. **29**(6), 969–993 (2009)
9. Arrizubieta, J.I., Klocke, F., Gräfe, S., Arntz, K., Lamikiz, A.: Thermal simulation of laser-assisted turning. Procedia Eng. **132**, 639–646 (2015)
10. Zhang, X.H., Wen, D.D., Deng, Z.H., Li, S., Wu, Q.P., Jiang, J.: Study on the grinding behavior of laser-structured grinding in silicon nitride ceramic. Int. J. Adv. Manuf. Technol. **96**(9–12), 3081–3091 (2018)
11. Chen, L., Siores, E., Wong, W.C.K.: Optimising abrasive waterjet cutting of ceramic materials. J. Mater. Process. Technol. **74**(1–3), 251–254 (1998)
12. Pawar, P., Ballav, R., Kumar, A.: An overview of machining process of alumina and alumina ceramic composites. Manuf. Sci. Technol. **3**(1), 10–15 (2015)
13. http://stjorsen.pl/wp-content/files/Katalog_Ceramika_NOWY_2016.pdf. Accessed 09 July 2018
14. http://www.cerel.eu/2.html. Accessed 22 Sept 2018
15. Gawlik, J., Krajewska, J., Niemczewska-Wójcik, M.: Precision machining of spherical ceramic parts. Adv. Manuf. Sci. Technol. **37**(4), 19–30 (2013)
16. https://www.sandvik.coromant.com/sitecollectiondocuments/downloads/global/brochures/pl-pl/c-2929-61.pdf. Accessed 09 July 2018
17. Musiał, W.: Investigation of ceramics material surface state after microgrinding process with nano feed-in. Arch. Mech. Technol. Autom. **29**(4), 11–19 (2009). (in Polish)
18. Wdowik, R., Porzycki, J., Magdziak, M.: Measurements of surface texture parameters after ultrasonic assisted and conventional grinding of ZrO_2 based ceramic material characterized by different states of sintering. Procedia CIRP **62**, 293–298 (2017)
19. Qu, S., Gong, Y., Yang, Y., Cai, M., Sun, Y.: Surface topography and roughness of silicon carbide ceramic matrix composites. Ceram. Int. **44**(12), 14742–14753 (2018)
20. https://www.ceramics.net/services/materials-engineering-expertise. Accessed 21 Sept 2018

21. Chen, C.C., Hsiang, H.I., Hsu, S.W.: Preparation and characterization of Y-TZP powders coated with alumina. J. Ceram. Process. Res. **9**(2), 131–134 (2008)
22. Masaki, T., Nakajima, K., Shinjo, K.: High-temperature mechanical properties of Y-PSZ HIPed under an oxygen-containing atmosphere. J. Mater. Sci. Lett. **5**(11), 1115–1118 (1986)
23. Sornakumar, T., Annamalai, V.E., Krishnamurthy, R., Gokularathnam, C.V.: Lapping of composite of Y-TZP and Ce-TZP. J. Mater. Sci. Lett. **13**(3), 187–189 (1994)
24. https://www.ceramtec.com/ceramic-materials/. Accessed 22 Sept 2018
25. https://www.azom.com/article.aspx?ArticleID=4537. Accessed 22 Sept 2018
26. http://ktwia.prz.edu.pl/projekt-badawczy-pbs2b6172013/. Accessed 14 Aug 2018